Title: Targeting DNA damage response promotes anti-tumor immunity through STING-mediated T-cell activation in small cell lung cancer

Authors: Triparna Sen[1], B. Leticia Rodriguez[1], Limo Chen[1], Carminia Della Corte[1], Naoto Morikawa[1@], Junya Fujimoto[2], Sandra Cristea[3.4], Thuyen Nguyen[3.4], Lixia Diao[5], Lerong Li[5,#], Youhong Fan[1], Yongbin Yang[1,†], Jing Wang[5], Bonnie S. Glisson[1], Ignacio I. Wistuba[2], Julien Sage[3.4], John V. Heymach[1,6], Don L. Gibbons[1,7], Lauren A. Byers[1]*

Author Affiliations: Departments of [1]Thoracic/Head and Neck Medical Oncology, [2]Translational Molecular Pathology, [5]Bioinformatics and Computational Biology, [6]Cancer Biology and [7]Molecular and Cellular Oncology, The University of Texas MD Anderson Cancer Center, Houston, TX 77030, USA; Departments of [3]Pediatrics and [4]Genetics, Stanford University, Stanford, CA 94305, USA.

*Correspondence to: Dr. Lauren A Byers, 1515 Holcombe Blvd, Unit 0432, Houston, Texas, 77030. **Email:** lbyers@mdanderson.org

[@] **Current address**: carcinoma@nifty.com

[#] **Current Address:** lerong.li@gmail.com

† **Current Address**: yybvsywz@163.com; Department of Obstetrics and Gynecology, Shanghai General Hospital, Shanghai, Shanghai 200080, China

Materials and Methods

Cell culture

Cell lines were grown in RPMI, unless otherwise mentioned by the provider, with 10% fetal bovine serum and antibiotics, cultured at 37°C in a humidified chamber with 5% CO_2. All cell lines included in the study were profiled at passage 4-8 to abrogate the heterogeneity introduced by long-term culture. All cell lines were tested for Mycoplasma as previously described and the characteristic phenotype (floating aggregates and colony formation) of small cell lung cancer (SCLC) cell lines.

Knockdown of *CHEK1, PARP, IRF3, TMEM173 (STING)*

SCLC cells were transfected with Validated Stealth Select RNAi siRNA *CHEK1, PARP, IRF3, STING* duplexes at a concentration of 10 nmol/L in Opti-MEM, or with Stealth RNAi Negative Universal Control using Lipofectamine 2000 (all from Invitrogen) according to the manufacturer's protocol. Seventy-two hours after transfection, the cells were subjected to drug treatments. The efficiency of the knockdown in all cases was confirmed by real-time reverse transcriptase PCR and western blot analysis.

Knockdown of *STING* and *MB21D1* (cGAS)

RPP/mTmG cells were transformed with Dharmacon *TMEM173* virus particle of shRNA (CloneID: V2LMM_103338), *MB21D1* virus particle of (CloneID: V2LMM_61275) and GIPZ Non-silencing Lentiviral shRNA Control (Catalog # RHS4348). Transformed clones were selected by puromycin. Knockdown was confirmed by real-time reverse transcriptase PCR and western blot analysis.

RNA isolation

RNA was isolated using the Direct-zol RNA MiniPrep Kit (Zymo Research, cat# R2050) according to the manufacturer's instructions. RNA concentrations were determined using a NanoDrop 2000 UV-Vis spectrophotometer (Thermo Scientific).

Reverse transcription

Reverse transcription reactions were carried out using SuperScript III First-Strand Synthesis SuperMix (Invitrogen, cat# 18080-400) according to the manufacturer's instructions.

Preparation of protein lysates

Protein lysate was collected from sub confluent cultures after 24-hr in full-serum media (10% fetal bovine serum [FBS]), serum-starved media (0% FBS), or serum-stimulated media (24 hr of 0% FBS followed by 30 min of 10% FBS immediately before lysis). For total protein lysate preparation, media were removed, and cells were washed twice withice-cold phosphate-buffered saline containing complete protease and PhosSTOP phosphatase inhibitor cocktail tablets (Roche Applied Science, Mannheim, Germany) and 1 mM Na3VO4. Lysis buffer (1% Triton X-100, 50 mM HEPES [pH 7.4],150 mM NaCl, 1.5 mM MgCl2, 1 mM EGTA, 100 mM NaF, 10 mM NaPPi, 10% glycerol,1 mM PMSF, 1 mM Na3VO4, and 10 μg/mL aprotinin). Samples were vortexed frequently on ice and then centrifuged. Cleared supernatants were collected and the protein was quantified using a BCA kit (Pierce Biotechnology).

Western blot analysis

Western blot analysis was performed using SDS-PAGE followed by transfer to nitrocellulose membrane using the BioRad Gel system. Membranes were incubated in the following primary antibodies (1:1000) overnight: PD-L1 (CST), total and phospho- (S366) STING (CST), total and phospho- (S172) TBK1 (CST), total and phospho- (S396) IRF3 (CST), cGAS (CST), Histone H3, pro and cleaved caspase 3, pro and cleaved caspase 9, Lamin B1 and Actin. Secondary antibodies

were purchased from BioRad, detected using the Li-CorOdyssey-499 Imager, and image-captured and quantitated using Image Studio Version 2.1 software.

Reverse-phase protein array (RPPA)

RPPAs were printed from lysates as previously described. The quality of the antibodies and validated by western blots and correlation of protein levels in previous RPPA experiments were determined, as previously described. The RPPA samples were analyzed as described before.

Tumor growth assessment

Flank syngeneic tumors were established as described above. Tumors were evaluated twice weekly for the duration of the study. B6129F1 mice with similar-sized tumors were identified. The length and width of tumors were measured manually with handheld slide calipers, and body weights of mice were measured using a bench top weighing scale. Tumor volume and body weights were measured on all mice three times per week and calculated (width^2 × length × 0.4). Once the average tumor size was in the range of 120-150 mm^3, mice were randomized into dosing groups using stratified sampling by assigning three animals per group for short-term reverse-phase protein array analysis and long-term treatment. The randomization process ensured that the average tumor volume for each dosing group was approximately equal at the beginning of the study and mice with differing tumor volumes were evenly distributed among the groups. Dosing schedules and duration varied depending on the study. Mice were weighed and tumors were measured three times per week for the duration of the study, and a decrease in body weight >15% was considered indicative of a toxic dose. The Student t-test was used to determine statistical significance between compound- and vehicle-treated groups.

Antibody-mediated cell depletion

Anti-CD8 antibody (2.43; BioXCell) or an immunoglobulin G (IgG) control was injected into the mice (200 µg, intraperitoneally) twice weekly for 2 weeks beginning on day 1 after a subcutaneous cancer cell injection.

Histologic analysis

Tissues were fixed in 10% paraformaldehyde and embedded in paraffin. Haematoxylin and eosin-stained sections were examined to identify micrometastases. For immunohistochemical, cryosections (8 µm) of tumour tissues were fixed with acetone and stained with antibody against mouse CD3 and CD8 and horseradish peroxidase-conjugated secondary antibody. Images ($\times$ 20) were acquired with an Olympus BX41 microscope.

Micronuclei Assay

Cells were cultured as discussed earlier and treated with or without prexasertib (1µM) or olaparib (10µM). Cytochalasin B was added at 20th hour to each culture to give a final concentration of 3 µg/ml and the culture was incubated at 37 °C for up to 24hrs. After 24hrs incubation, the cells were centrifuged at 1000 rpm for 5 min. The supernatant was removed and the pellet was treated with weak hypotonic solution (0.075 M KCl/0.9 % Saline, 1:9) and incubated at 37 °C for 5 min. After this, the cells were centrifuged and the pellets were fixed in fresh fixative (methanol:acetic acid, 3:1). Cells were dropped onto glass slides were prepared and stained with ProLong® Gold Antifade Mountant with DAPI for scoring. At least 1000 multinucleated cells, following the standard specifications, were scored for each slides.

Statistics

Flow cytometry statistical analyses were performed with GraphPad Prism 5.0 software. Significant differences (p<0.05) between two groups were identified by Student's t-tests.

Figures and Figure Legends:

Figure S1

A

H82 — Con | SCR | *CHEK1* KD
H446 — Con | SCR | *CHEK1* KD

PD-L1

Actin

H82   H446

B

SCR | *PARP* KD | SCR | *PARP* KD

PD-L1

Actin

H526   H1048

C

LY2603618   Con | 48 | 72   Con | 48 | 72 (h)

PD-L1

Actin

H82   H524

D

Control   Olaparib   Prexasertib

2.5μm   2.5μm   2.5μm

E

H69   H446   mTmG

Number of Micronuclei

Control | Olaparib | Prexasertib

F

RPP (spontaneous)

p<0.001

PD-L1 protein expression

Veh | 1d | 3d | 7d

Prexasertib treatment

G CD3+ total T-cells

%CD3+ cells

***

Veh   1d   7d
Prexasertib treatment

H CD8+ cytotoxic T-cells

%CD8+ cells

**

Veh   1d   7d
Prexasertib treatment

I CD4+ helper T-cells

%CD4+ cells

**

Veh   1d   7d
Prexasertib treatment

J Exhausted T-cells

%PD1%/TIM3 cells

***

Veh   1d   7d
Prexasertib treatment

K Naive T-cells

%CD44medium/CD62Lhigh

***

Veh   1d   7d
Prexasertib treatment

L Memory/Effector T-cells

%CD44high/CD62Llow

**   ***

Veh   1d   7d
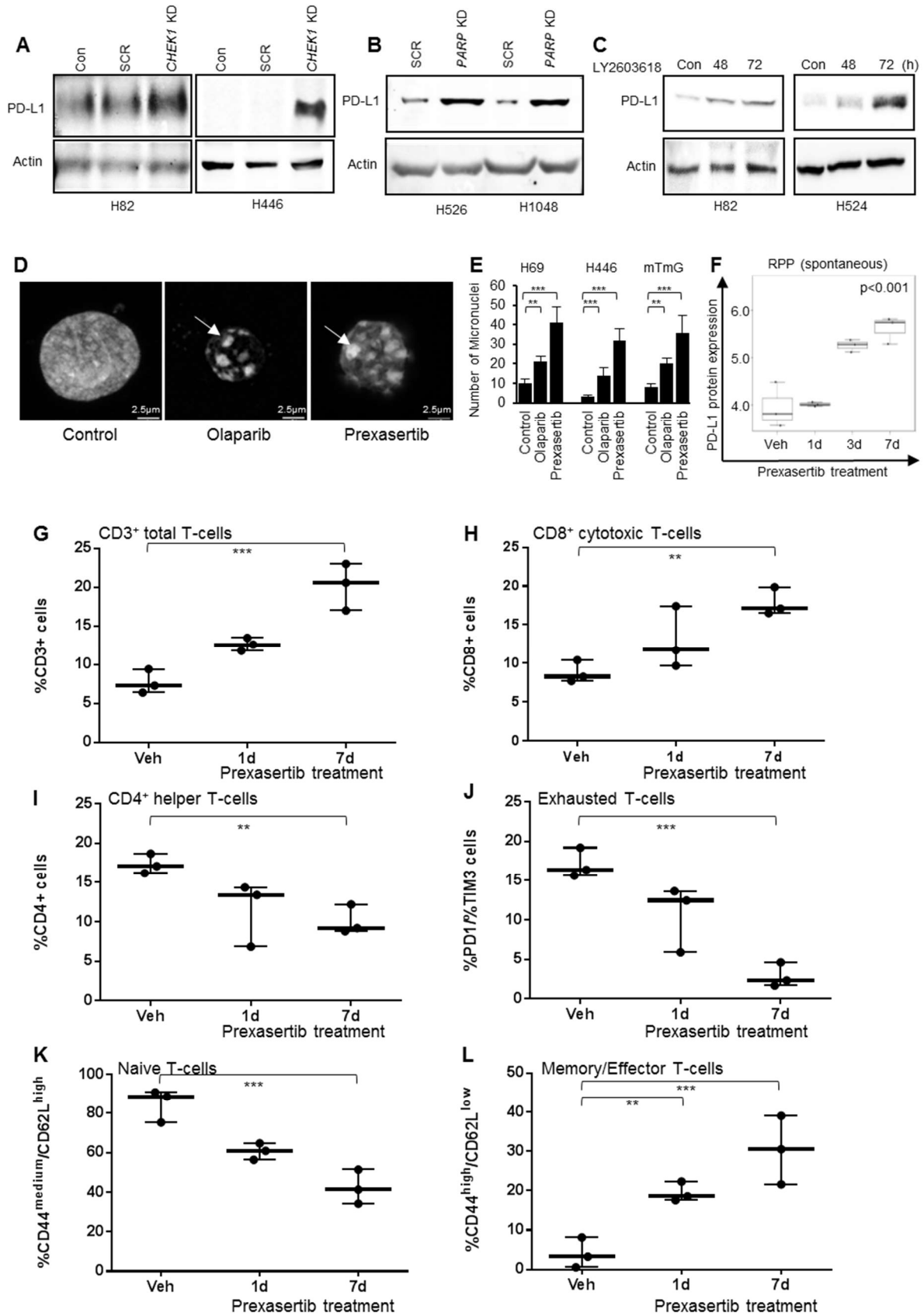Prexasertib treatment

7

Figure S1: DNA damage response (DDR) targeting enhances PD-L1 protein expression in vitro and in vivo and enhances immune response in small cell lung cancer (SCLC).

(A-B) SCLC cells as indicated were transfected with (A) *CHEK1*-knockdown (KD) or (B) *PARP*-KD siRNA or scrambled control (SCR). Protein extracts were subjected to immunoblot analysis for PD-L1. Actin served as a loading control.

(C) SCLC cells were treated with a second CHK1 inhibitor, LY2603618, for 48 and 72 hours and protein extracts were subjected to immunoblot analysis for PD-L1 expression. Actin served as a loading control.

(D-E) Representative images showing micronuclei after olaparib and prexasertib treatment, as compared to untreated control, in H69 cells following DAPI staining (D). (E) Quantification of cells containing micronuclei (MN) reveals increase of MN after DDR inhibition. Results were obtained in H69, H446 and RPP/mTmG cells untreated or treated with olaparib (10μM) or prexasertib (1μM) for 24 hours.

(F) The genetically engineered SCLC RPP (spontaneous) mouse model harboring conditional loss of Trp53, p130, and Rb1 was treated with single-agent prexasertib (10 mg/kg twice per day) for 1, 3, and 7 days. Proteomic analysis of tumor lysates demonstrated a time-dependent increase in PD-L1 protein expression after treatment with prexasertib.

(G-L) Lung tissues were collected at day 1 (1d) and day 7 (7d) for fluorescence-activated cell sorting (FACS) analysis. The percentage of lung-infiltrating T-cells among total $CD3^+CD45^+$ T-cells (G), cytotoxic $CD8^+$ T-cells (H), $CD4^+$ helper T-cells (I), $PD1^+TIM3^+$ exhausted T-cells (J), $CD44^{low}CD62L^{high}$ naïve T-cells (K), and $CD44^{high}CD62L^{low}$ memory/effector T-cells (L) was determined by flow cytometry. All data represent at least two independent experiments.

**p < 0.01 and ***p < 0.0001.

Figure S2
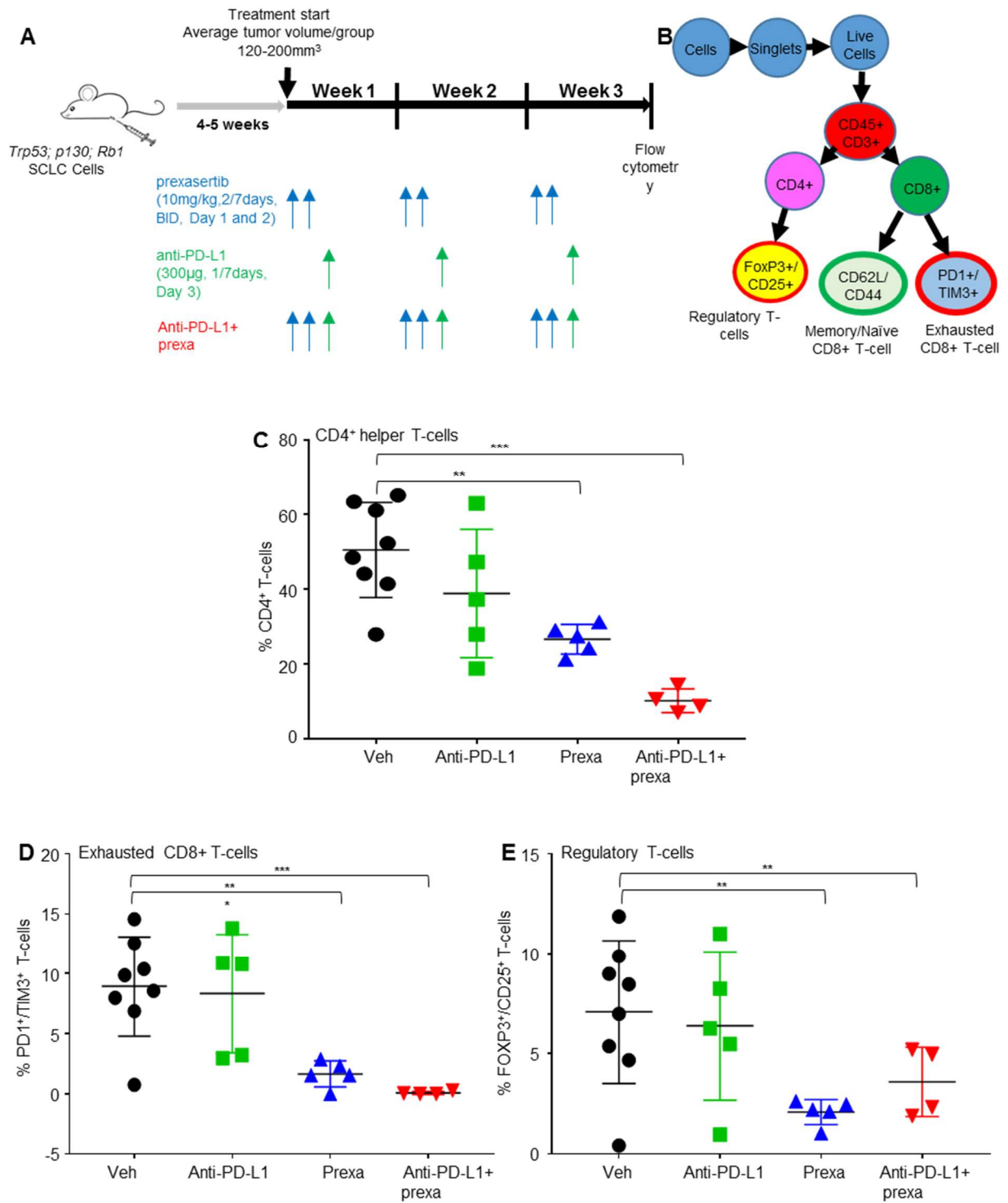
Figure S2: Analysis of immune infiltrates of tumors after CHK1 inhibition.

(A) Tumor growth time and dosing schedule for RPP/mTmG flank model treated with IgG, prexasertib alone (10 mg/kg twice per day, days 1-2 of 7 days), anti-PD-L1 alone (300 µg, day 1 of 7 days) and combination.

(B) Gating strategy of tumors FACS analysis.

(C-E) SCLC tumors showed in Figure 1H were harvested at day 21 and immune profiling was analyzed by FACS at the endpoint; the cumulative data for all tumors is shown. FACS results for (C) CD4$^+$ helper T-cells (CD45$^+$CD3$^+$CD4$^+$), (D) exhausted T-cells (CD45$^+$CD3$^+$CD8$^+$PD-1$^+$TIM3$^+$) and (E) regulatory T-cells (CD45$^+$CD3$^+$CD4$^+$CD25$^+$Foxp3$^+$) are also shown for the endpoint primary tumors. The statistical summary is shown with ANOVA test. ns, no significance; *, $p < 0.05$; **, $p < 0.001$; ***, $p < 0.0001$.

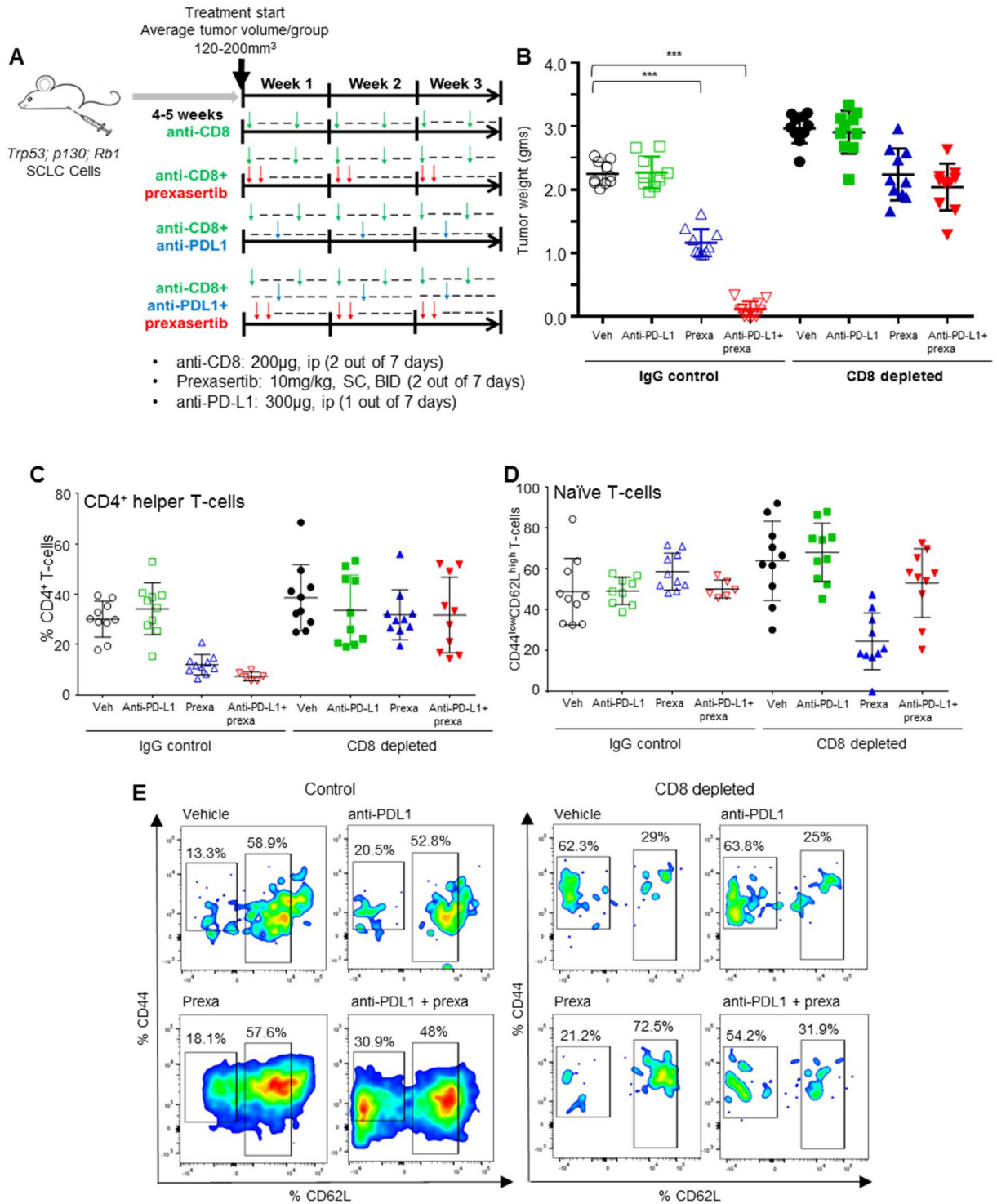**Figure S3**

A

Treatment start
Average tumor volume/group
120-200mm³

Trp53; p130; Rb1
SCLC Cells

4-5 weeks

| | Week 1 | Week 2 | Week 3 |

anti-CD8

anti-CD8+
prexasertib

anti-CD8+
anti-PDL1

anti-CD8+
anti-PDL1+
prexasertib

- anti-CD8: 200µg, ip (2 out of 7 days)
- Prexasertib: 10mg/kg, SC, BID (2 out of 7 days)
- anti-PD-L1: 300µg, ip (1 out of 7 days)

B

Tumor weight (gms)

*** ***

Veh Anti-PD-L1 Prexa Anti-PD-L1+prexa   Veh Anti-PD-L1 Prexa Anti-PD-L1+prexa

IgG control   CD8 depleted

C % CD4⁺ helper T-cells

% CD4⁺ T-cells

Veh Anti-PD-L1 Prexa Anti-PD-L1+prexa   Veh Anti-PD-L1 Prexa Anti-PD-L1+prexa

IgG control   CD8 depleted

D Naïve T-cells

CD44^low CD62L^high T-cells

Veh Anti-PD-L1 Prexa Anti-PD-L1+prexa   Veh Anti-PD-L1 Prexa Anti-PD-L1+prexa

IgG control   CD8 depleted

E

Control   CD8 depleted

Vehicle   anti-PDL1   Vehicle   anti-PDL1
13.3% 58.9%   20.5% 52.8%   62.3% 29%   63.8% 25%

Prexa   anti-PDL1 + prexa   Prexa   anti-PDL1 + prexa
18.1% 57.6%   30.9% 48%   21.2% 72.5%   54.2% 31.9%

% CD44   % CD44

% CD62L   % CD62L

Figure S3: CD8+ T-cells are required for anti-tumor immunity induced by CHK1 inhibition with or without PD-L1 blockade.

(A) Tumor growth time and dosing scheme of CD8 depletion in the RPP/mTmG B6129 flank mouse model. Mice were treated with vehicle, prexasertib alone (10 mg/kg twice per day, days 1-2 of 7 days), anti-PD-L1 alone (300 µg, day 1 of 7 days), or prexasertib+anti-PD-L1 either with or without anti-CD8 antibody (200 µg, days 1-2 of 7 days).

(B) Tumor weight (g) in mice treated with vehicle, prexasertib alone (10 mg/kg twice per day, days 1-2 of 7 days), anti-PD-L1 alone (300 µg, day 1 of 7 days), or prexasertib+anti-PD-L1 either with or without anti-CD8 antibody (200 µg, days 1-2 of 7 days).

(C-E) SCLC tumors in Figure 3A were harvested at day 21 and immune profiling was analyzed by FACS at the endpoint; representative plots and cumulative data for all tumors are shown. Results are shown for (C) CD4$^+$ helper T-cells (CD45+CD3+CD4+), (D, E) naïve T-cells (CD45$^+$CD3$^+$CD8$^+$CD44^{low}CD62L^{high}) from the endpoint primary tumors. The statistical summary is shown with ANOVA test. ns- no significance; *, $p < 0.05$; **, $p < 0.001$; ***, $p < 0.0001$.

Figure S4

A

Trp53; p130; Rb1 SCLC Cells

Treatment start
Average tumor volume/group 120-200mm³

4-5 weeks | Week 1 | Week 2 | Week 3 | **Continued treatment long term**

Olaparib (50 mg/kg, 5 out of 7 days)

anti-PD-L1 (10mg/kg, 3 out of 7 days)

Combination

B

Trp53; p130; Rb1 SCLC Cells

Treatment start
Average tumor volume/group 120-200mm³

4-5 weeks | Week 1 | Week 2 | Week 3 | **Flow cytometry performed on resected tumors**

Olaparib (50 mg/kg, 4 out of 7 days)

anti-PD-L1 (300µg, 1 out of 7 days)

Combination

C

RPP (B6129) [reduced dose]

- Vehicle
- anti-PD-L1
- Olaparib
- Combination

Tumor volume (mm³±SEM)

***
**

Days elapsed

D

Tumor volume (mm)

Vehicle | Anti-PD-L1 | Olaparib | Combination

Days elapsed

E

PD-L1 protein expression

p<0.0001; FC=1.47

Vehicle | Olaparib
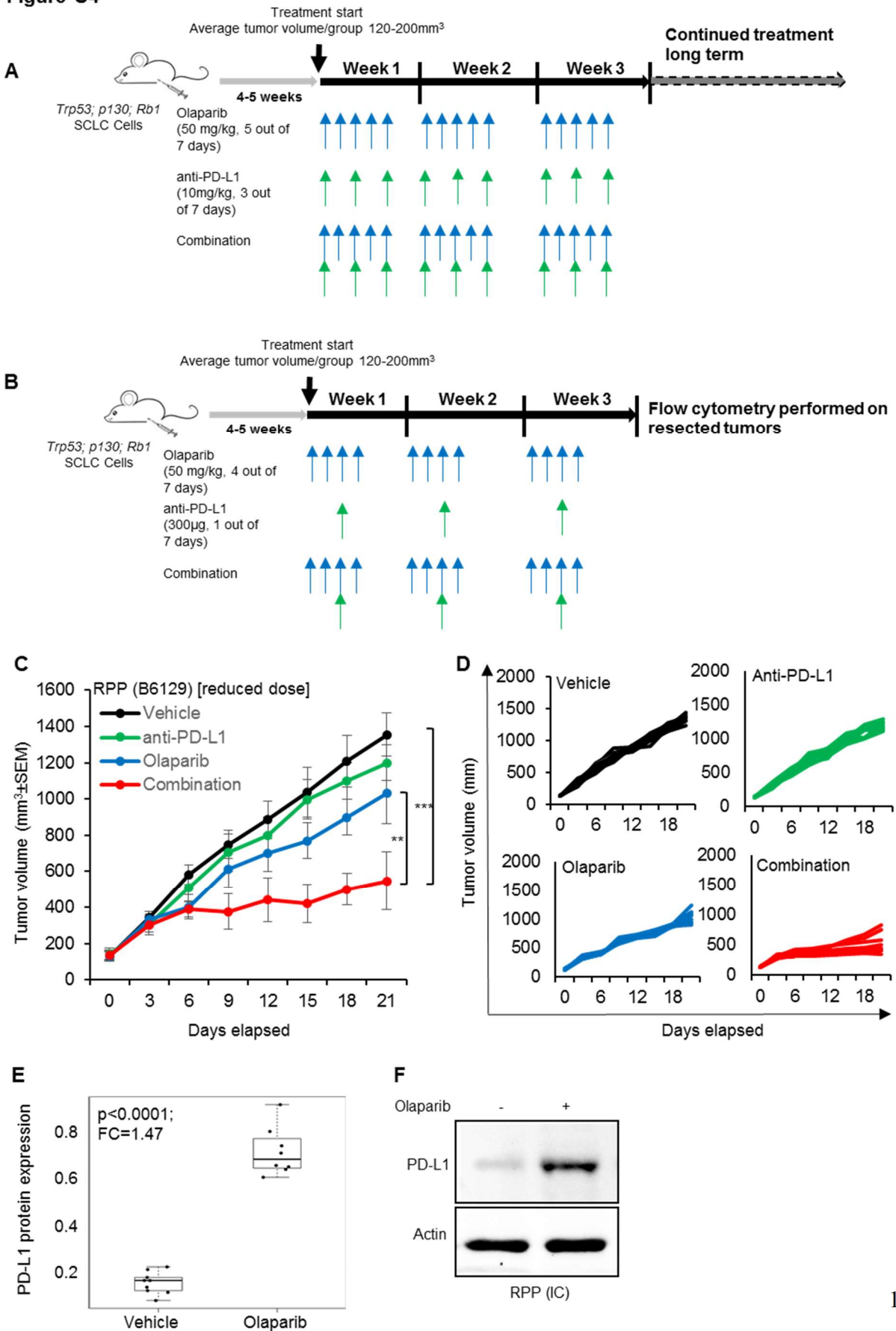
F

Olaparib   −   +

PD-L1

Actin

RPP (IC)

13

Figure S4: PARP inhibition augments anti-PD-L1 antibody-induced antitumor immunity.

(A) Tumor growth time and dosing scheme of RPP/mTmG B6129 flank mouse model. Mice were treated with vehicle, olaparib alone (50mg/kg, 5 out of 7 days), anti-PD-L1 alone (10mg/kg, 3 of 7 days), or olaparib+anti-PD-L1 for 80 days.

(B) Tumor growth time and dosing scheme of RPP/mTmG B6129 flank mouse model for a lower dosing schedule. Mice were treated with vehicle, olaparib alone (50mg/kg, 4 out of 7 days), anti-PD-L1 alone (300μg, 1 of 7 days), or olaparib+anti-PD-L1 for 21 days. Tumors resected at the end of the study for flow cytometry.

(C-D) B6129F1 mice were injected with murine RPP derived from small cell lung cancer in a genetically engineered mouse model with conditional loss of *Trp53*, *p130*, and *Rb1*. Tumor growth curves ± standard error of the mean (SEM) (A) and for each individual mouse (B) are shown for mice treated with IgG (300 μg, day 1 of 7 days), anti-PD-L1 (300 μg, day 1 of 7 days), olaparib (50 mg/kg, days 1-4 of 7 days), or the combination of olaparib+anti-PD-L1 (n = 10 per group) for 21 days.

(E) Treatment with olaparib enhanced PD-L1 protein expression in RPP flank tumors as measured by reverse phase protein array (RPPA) analysis (fold change (FC)=1.47; p<0.0001).

(F) Western blot analysis confirmed increased PD-L1 protein expression after treatment with olaparib in immunocompetent (IC) mice in the RPP B6129 flank model , as shown in Fig. S4C.

Figure S5

A RPP spontaneous (4mo)

500um 100um

B

p=0.969

Baseline tumor burden

Vehicle Anti-PD-L1 Olaparib Combination

C CD3+ total T-cells

% CD3⁺ T-cells

**

Vehicle Anti-PD-L1 Olaparib Combination

D

Vehicle Anti-PD-L1
Olaparib Combination

13.7% 14.4%
13.6% 52.2%

CD3⁺ / CD45⁺

E CD8+ cytotoxic T-cells

% CD8⁺ T-cells

*

Vehicle Anti-PD-L1 Olaparib Combination

F

Vehicle Anti-PD-L1
Olaparib Combination

19.4% 0.53%
14.1% 1.79%
8.77% 0.46%
2.11% 8.24%

CD4⁺ / CD8⁺

G CD4⁺ helper T-cells

% CD4⁺ T-cells

**

Vehicle Anti-PD-L1 Olaparib Combination

H Exhausted T-cells

% PD1⁺/TIM3⁺ T-cells

*

Vehicle Anti-PD-L1 Olaparib Combination

I

Vehicle Anti-PD-L1
Olaparib Combination

1.34% 14.9%
4.73% 0.31%

TIM3⁺ / PD1⁺

J Regulatory T-cells

% FOXP3⁺/CD25⁺ T-cells

*

Vehicle Anti-PD-L1 Olaparib Combination

K

Vehicle Anti-PD-L1
Olaparib Combination

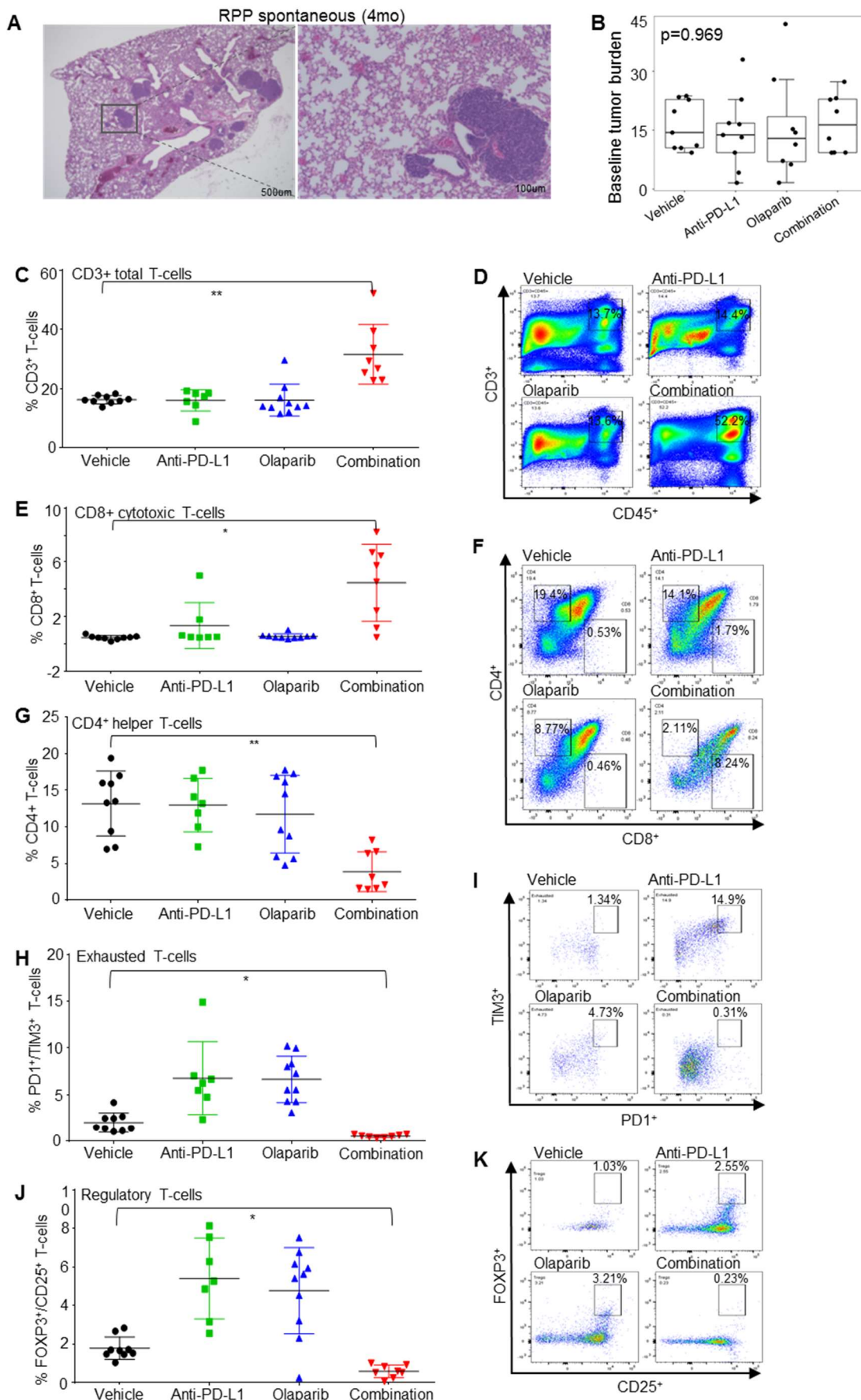1.03% 2.55%
3.21% 0.23%

FOXP3⁺ / CD25⁺

15

Figure S5: PARP inhibition augments anti-PD-L1 antibody-induced antitumor immunity in a SCLC spontaneous mouse model:

(A) H and E staining of the lungs of pre-treated RPP spontaneous model at 4 months after Ad-CMV-Cre administration demonstrating appreciable tumor burden at this time.

(B) Baseline tumor burden (as measured by luciferase imaging) to ensure comparable tumor burden between treatment groups in RPP spontaneous model.

(C-K) SCLC tumors showed in Figure 4C were harvested at Day 21 and the immune profiling was analyzed by FACS at the endpoint, the representative plots and cumulative data for all the tumors were shown. FACS analysis of CD3+CD45+ total T-cells (C-D), CD3+CD45+CD8+ cytotoxic T-cells (E-F), CD4$^+$ helper T-cells (G); CD45$^+$CD3$^+$CD8$^+$PD-1$^+$TIM3$^+$ exhausted T-cells (H-I); and CD45$^+$CD3$^+$CD4$^+$CD25$^+$Foxp3$^+$ regulatory T-cells (J-K) from the endpoint primary tumors. The statistical summary was done with ANOVA test. ns, no significance; *, $p<0.05$; **, $p<0.001$; ***, $p<0.0001$.

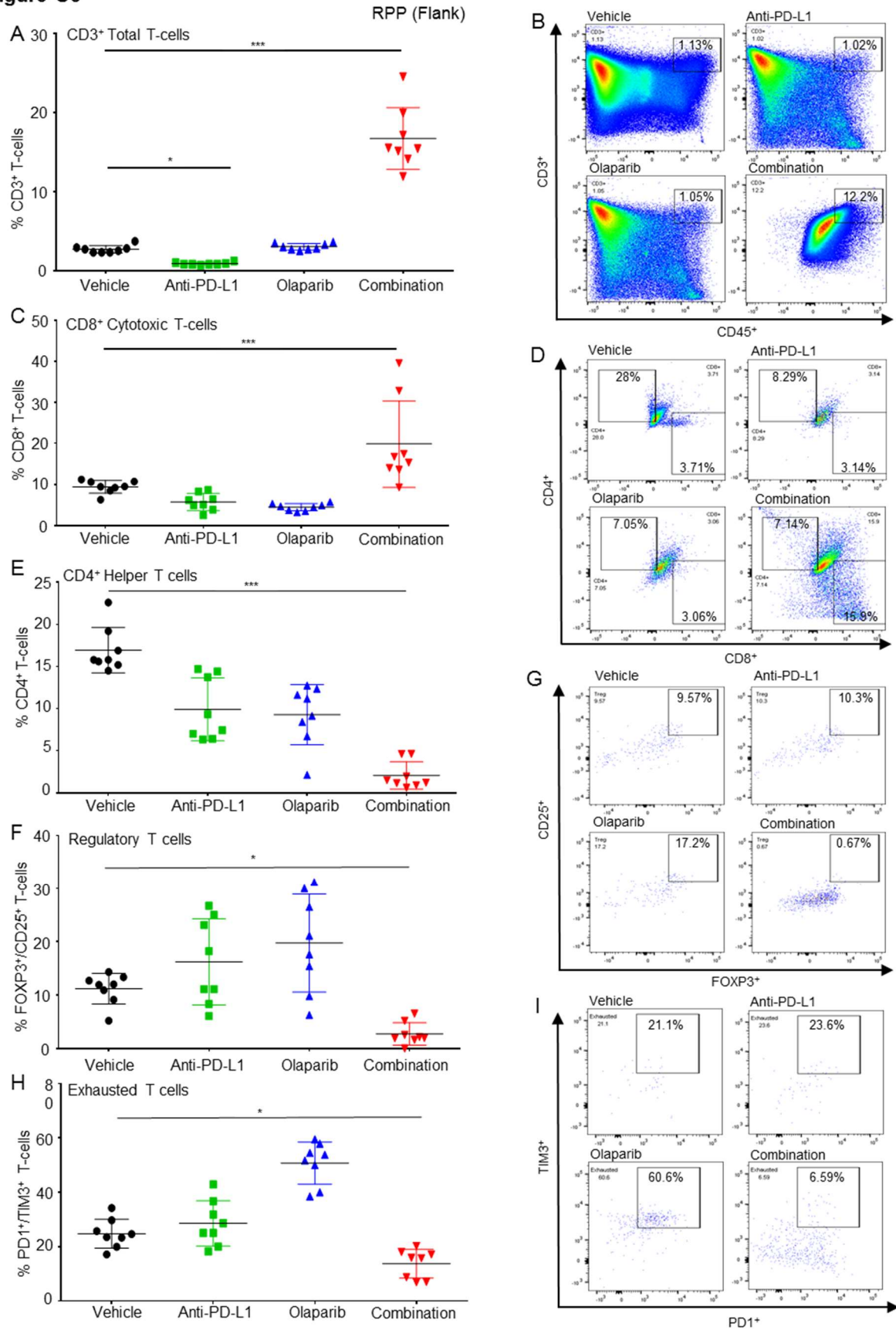**Figure S6**

RPP (Flank)

Figure S6: PARP inhibition augments anti-PD-L1 antibody-induced antitumor immunity in a RPP/mTmG flank model.

(A-I) SCLC tumors in Figure S4C were harvested at Day 21 and the immune profiling was analyzed by FACS at this endpoint, the representative plots and cumulative data for all the tumors are shown. FACS analysis of CD3+CD45+ Total T-cells (A-B), CD3+CD45+CD8+ cytotoxic T-cells (C-D), CD3+CD45+CD4+ helper T-cells (E), CD45$^+$CD3$^+$CD4$^+$CD25$^+$Foxp3$^+$ T-regulatory cells (F-G), CD45$^+$CD3$^+$CD8$^+$PD-1$^+$TIM3$^+$ exhausted CD8+ T cells (H-I) from the endpoint primary tumors are shown. The statistical summary was done with ANOVA test. ns, no significance; *, $p < 0.05$; **, $p < 0.001$; ***, $p < 0.0001$.
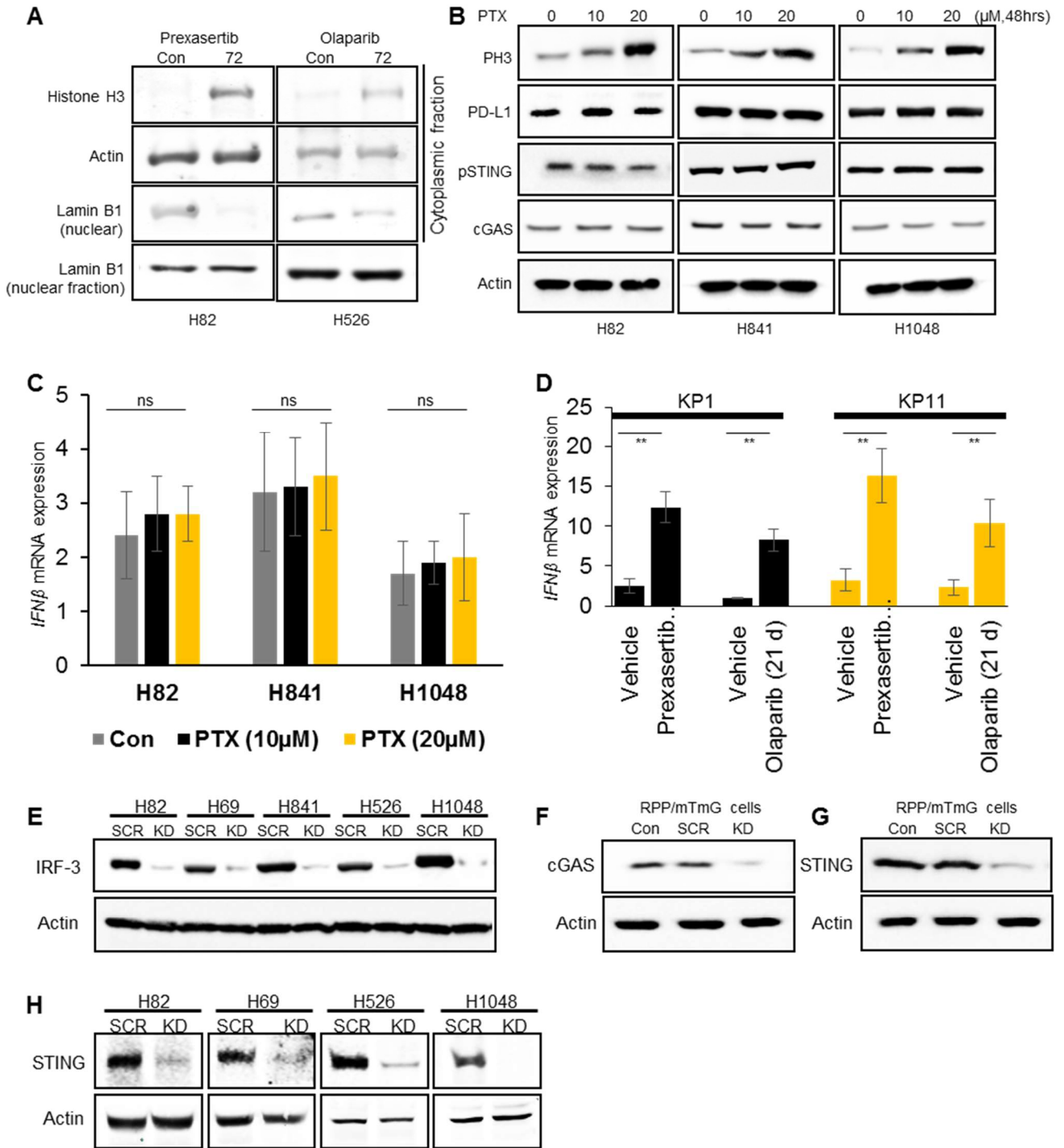
Figure S7

Figure S7: Role of STING pathway in DDR-targeting dependent anti-tumor response.

(A) Immunoblot of Histone H3 in the cytosolic fraction of SCLC cells treated with prexasertib (left panel) or olaparib (right panel). Actin was used as a loading control. Nuclear Lamin B1 shows the degree of fractionation achieved. Lamin B1 was the loading control for the nuclear fraction.

(B-C) Immunoblot analysis (B) and *IFNβ* mRNA expression as measured by qPCR (C) of SCLC cell lines (H82, H841, H1048) treated with a drug that does not induce DDR, paclitaxel (PTX) (10 and 20μM for 48 hours) to assess the expression of PD-L1, pSTING_S366 and cGAS. Phospho-histone H3 was assessed to demonstrate ongoing cell division and actin used as loading control.in panel B.

(D) Quantitative PCR (qPCR) measurement of *IFNβ* mRNA expression after treatment with prexasertib and olaparib in RPP/KP11 and RP/KP1 flank SCLC *in vivo* models.

(E) *IRF3* was knocked down (KD) in SCLC cells using *IRF3* siRNA normalized to a scrambled (SCR) siRNA control. Immunoblot analysis of IRF3 expression was used to confirm knockdown in these cells. Actin was used as a loading control.

(F-G) *cGAS* and *STING* were knocked down (KD) in SCLC RPP/mTmG cells using lentivirus and normalized to a scrambled (SCR) control. Immunoblot analysis of cGAS (F) or STING (G) expression was used to confirm knockdown in these cells prior to injection into mice. Actin was used as a loading control.

(H) *STING* was knocked down in SCLC cells using *STING* siRNA normalized to a scrambled (SCR) siRNA control. Immunoblot analysis of STING expression to confirm knockdown in these cells. Actin was used as loading control.

Table S1: The genotypic status of human SCLC cell lines

Cell Line	*MYCL* Copy Number (qPCR)	*cMYC* Copy Number (qPCR)	*MYCN* Copy Number (qPCR)	TP53 Mutation	*RB1* Status (qPCR)
H146	No Amp	No Amp	No Amp	Yes	loss
H446	No Amp	Amp	No Amp	Yes	loss
H524	No Amp	Amp	No Amp	Yes	loss
H2107	Amp	No Amp	No Amp	Yes	loss
H209	No Amp	No Amp	No Amp	Yes	loss
H1672	No Amp	No Amp	No Amp	Yes	WT
H1836	Amp	No Amp	No Amp	-	-
H1618	-	-	-	Yes	loss
H1417	No Amp	No Amp	No Amp	Yes	loss
H345	No Amp	No Amp	No Amp	Yes	WT
DMS53	-	-	-	Yes	WT
H2227	No Amp	No Amp	No Amp	Yes	loss
H865	No Amp	No Amp	No Amp	Yes	-
H1092	No Amp	No Amp	No Amp	Yes	WT
H526	No Amp	No Amp	Amp	Yes	loss
H82	No Amp	Amp	No Amp	Yes	loss
H1930	No Amp	No Amp	No Amp	Yes	WT
H69	No Amp	No Amp	Amp	Yes	loss
H2171	No Amp	Amp	No Amp	Yes	loss
DMS79	No Amp	No Amp	No Amp	Yes	loss
DMS153	-	-	-	Yes	loss
H889	Amp	No Amp	No Amp	Yes	WT
DMS114	-	-	-	Yes	WT
H841	No Amp	No Amp	No Amp	Yes	-
H2330	No Amp	No Amp	No Amp	-	-
H1048	-	-	-	Yes	-

Table S2: Primers sequences

Gene	Sense	Antisense
CHEK1	ATATGAAGCGTGCCGTAGACT	TGCCTATGTCTGGCTCTATTCTG
PARP	TGCAATGGTCGTGAACAACCT	CAACTGGGACCGTTGAAACTG
IRF3	AGAGGCTCGTGATGGTCAAG	AGGTCCACAGTATTCTCCAGG
STING	CCAGAGCACACTCTCCGGTA	CGCATTTGGGAGGGAGTAGTA
CXCL10	GTGGCATTCAAGGAGTACCTC	TGATGGCCTTCGATTCTGGATT
CCL5	CCAGCAGTCGTCTTTGTCAC	CTCTGGGTTGGCACACACTT
GAPDH	AGGGGAGATTCAGTGTGGTG	GGCCTCCAAGGAGTAAGACC
STING (murine)	TCGCACGAACTTGGACTACTG	CCAACTGAGGTATATGTCAGCAG
cGAS	CACGAAGCCAAGACCTCCG	GTCGCACTTCAGTCTGAGCA

Table S3: List of antibodies used for flow cytometry

Si. No	Antibody	Color	Company	Cat#	Clone
1.	CD62L	FITC	E-BIOSCIENCES	11-0621-85	MEL-14
2.	FOXP3	PerCp Cy5.5	E-BIOSCIENCES	45-5773-821	FJK-16s
3.	TIM3	PE	BIOLEGEND	134004	B8.2C12
4.	CD3	PE/DAZZLE	BIOLEGEND	100246	17A2
5.	CD8	PE/Cy7	BIOLEGEND	100722	53-6.7
6.	CD44	APC	BIOLEGEND	10311	1M7
7.	CD4	APC/Cy7	BIOLEGEND	100526	RM4-5
8.	CD45	PACIFIC BLUE	BIOLEGEND	103126	30-F11
9.	PD-1	BV605	BIOLEGEND	35220	29F.1A12
10.	CD69	BV650	BIOLEGEND	104541	H1.2F3
11.	CD25	BUV395	BD BIOSCIENCES	564022	PC61